Dalton Transactions

ROYAL SOCIETY OF CHEMISTRY

PAPER

View Article Online
View Journal | View Issue

Cite this: *Dalton Trans.*, 2026, **55**, 6453

Aluminum dihydride from E(IV) precursors (E = Si, Ge) and its bond-activation reactivities

Hemant Kumar,[a] Steven P. Kelley,[a] Tanya Batra,[b] Selvarajan Nagendran[b] and Justin R. Walensky *[a]

Received 25th February 2026,
Accepted 1st April 2026

DOI: 10.1039/d6dt00474a

rsc.li/dalton

A distinctive synthetic route has been demonstrated in which the aminotroponiminato (ATI)-stabilized aluminum dihydride complex [(ATI)AlH_2] was prepared from a [(ATI)$SiHCl_2$] precursor. [(ATI)AlH_2] was also isolated from aluminum(III) dichloride [(ATI)$AlCl_2$] *via* salt-metathesis reaction. Subsequent reaction with the ATIH ligand enabled the isolation of the *N*-tetracoordinated (ATI)Al(III)-complex *via* aluminum monohydride [(ATI)AlH(ATI)] intermediate. The dihydride compound was found to activate C=S (in CS_2) and P=Se (in Ph_3P=Se) bonds yielding the aluminum(III) μ-sulphide and μ-selenide dimer [(ATI)Al(μ-S)]$_2$ and [(ATI)Al(μ-Se)]$_2$, respectively. All compounds were characterized using multinuclear NMR spectroscopy and single-crystal X-ray diffraction.

Introduction

Main-group metal hydrides constitute a diverse and fundamentally important class of compounds with broad relevance in catalysis, small-molecule activation, and energy storage.[1–7] Among these, N-heterocyclic aluminum hydrides have emerged as a notable subclass, demonstrating utility in catalytic transformations and small-molecule activation.[3,8–13] These compounds typically feature a terminal or bridging hydride bound to an aluminum centre that is stabilized by N-heterocyclic ligand frameworks such as amidinates, β-diketiminates, or pincer-type ligands.[8,10–34] While most studies on aluminum hydrides have focused on systems supported by amidinate and β-diketiminate ligands, there remains significant scope to explore alternative ligands.

To the best of our knowledge, synthetic strategies that employ group-14 precursors (LEX_3; E = Si or Ge) for the preparation of aluminum dihydrides have not yet been established. Our group has previously shown that treatment of $H_2Ge(3,5\text{-}(CF_3)_2C_6H_3)$ with [$(C_5Me_5)_2U(CH_3)(I)$], Scheme 1,[35] can afford a compound with a uranium–germanium bond. To create other such starting materials, we targeted group 14 trihydride compounds of the form (ATI)$E(H)_3$, (ATI) = ^{i}Bu-substituted aminotroponiminate; E = Si, Ge. We recently reported the isolation of (ATI)-stabilized trichloro silane and germane compounds.[36] While we now tried to convert these compounds to their respective trihydrides by adding $LiAlH_4$, the result was an *aluminum* dihydride, [(ATI)AlH_2].

In this context, ATI ligands present an attractive yet underexplored ligand for aluminum hydride stabilization. To date, only one example of an ATI-supported aluminum hydride, [$(^iPr)_2$ATI]AlH_2, has been reported,[37] but its reactivity remains unexplored. Aluminum dihydride complexes of the type $LAlH_2$ (L = monoanionic ligand) are typically synthesized either *via* protonolysis of alane adducts ($R_3N{\cdot}AlH_3$) with the corresponding ligand (LH) or *via* hydride substitution of $LAlX_2$ (X = halide) precursors. Further, N-heterocyclic aluminum complexes containing heavier chalcogens and featuring Al_2E_2 cores (E = S, Se, Te) have generally been synthesized using elemental chalcogens or chalcogen-transfer reagents such as R_3P=E.[32,38–43] Notably, in 2019 Cabrera and co-workers reported, [{^{Me}LAl(μ-S)}$_2$], containing a four-membered Al_2S_2 ring, through the activation of CS_2 by $^{Me}LAlH_2$ (^{Me}L = HC[(CMe)N(2,4,6-$Me_3C_6H_2$)]$_2$).[44] This shows the ability of N-heterocyclic aluminum dihydride to activate CS_2 which can be a useful model for CO_2 reactivity or activation. Thus, in this contribution, apart from reporting the synthesis of ATI-stabil-

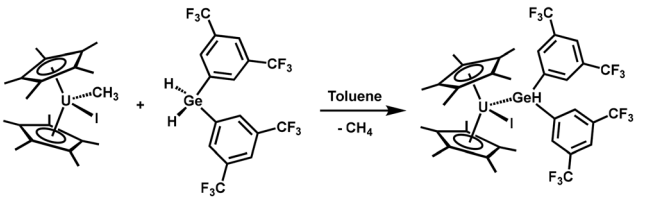

Scheme 1 Formation of a U–Ge bond through protonolysis of a U(IV)–methyl with a disubstituted germane.

[a]*Department of Chemistry, University of Missouri, Columbia, Missouri 65211, USA. E-mail: walenskyj@missouri.edu*
[b]*Department of Chemistry, Indian Institute of Technology Delhi, Hauz Khas, New Delhi 110016, India*

ized aluminum dihydride [(ATI)AlH_2] from a novel synthetic route starting from [(ATI)$SiHCl_2$] **1**, we also investigated the ability of the dihydride, **2**, to activate C═S and P═Se bonds.

Results and discussion

Synthesis and spectra

Aminotroponimine (ATIH) was deprotonated with *n*-BuLi, followed by reaction with an equimolar amount of trichlorosilane ($SiCl_3H$), yielding the ATI-stabilized dichlorosilane [(ATI)$SiCl_2H$] **1** in 85% isolated yield (Scheme 2). Compound **1** is readily soluble in toluene, THF, and chloroform, but insoluble in pentane. The complex was characterized by multinuclear NMR spectroscopy, infrared (IR) spectroscopy, and single-crystal X-ray diffraction. The ^{1}H NMR spectrum of **1** displayed the expected resonances. The methyl protons appeared as a doublet at δ = 0.82 ppm, while the methine and methylene protons were observed as a multiplet (δ = 2.06–2.00 ppm) and a doublet (δ = 3.61 ppm), respectively. The five protons of the seven-membered ATI backbone exhibited a triplet, doublet, and pseudo-triplet in a 1 : 2 : 2 intensity ratio at δ = 6.70, 6.56, and 6.30 ppm. The Si–H hydride resonance appeared as a singlet at δ = 7.05 ppm. The ^{13}C NMR spectrum of compound **1** showed seven distinct signals: three in the aliphatic region corresponding to the isobutyl substituents and four in the aromatic region attributable to the seven-membered ATI-ring. In the ^{29}Si NMR spectrum, compound **1** exhibits a doublet at δ = −88.0 ppm, which is shifted downfield relative to [(ATI)$SiCl_3$] (δ = −95.5 ppm) and is consistent with closely related dichlorosilane species reported in the literature;[45–49] for example, [Ph_2P(NDipp)$_2$]$SiHCl_2$, Dipp = 2,6-^{i}Pr$_2$C$_6$H$_3$, resonates at δ = −89.4 ppm.[49] The IR spectrum of compound **1** displays two Si–H stretching bands at ν = 2357 and 2338 cm^{-1} consistent with the analogous systems such as [PhC{(N^{t}Bu)(NDipp)}]$SiHCl_2$.[50]

To synthesize N-heterocyclic silane [(ATI)SiH_3], the reaction of compound **1** was carried out with $LiAlH_4$, which led to the unusual reactivity and afforded [(ATI)AlH_2], **2**, as a product (with 68% yield) instead of [(ATI)SiH_3]. Compound **2** is soluble in pentane, toluene, and THF. Similar reactions starting with [(ATI)$SiCl_3$] or [(ATI)$GeCl_3$] also afforded compound **2** with 80% yield (Scheme 3). Compound **2** was characterized using multinuclear NMR-spectroscopy, IR spectroscopy, and single-crystal X-ray diffraction techniques. The ^{1}H NMR spectrum of compound **2** gave the anticipated results; the resonance of methyl protons appeared as a doublet (δ = 0.92 ppm). Methine

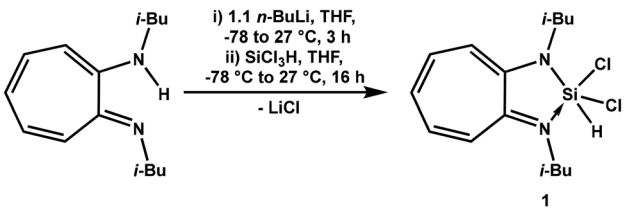

Scheme 2 Synthesis of ATI-stabilized dichlorosilane **1**.

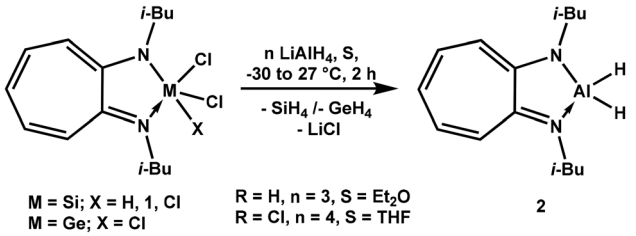

Scheme 3 Synthesis of ATI-stabilized Aluminium(III) dihydride **2**.

and methylene protons appeared as a multiplet (δ = 2.13–2.19 ppm) and a doublet (δ = 3.00 ppm), respectively. The Al–*H* hydride appeared as a singlet (δ = 5.06 ppm). The five protons of the seven-membered ring appear as triplet, doublet, and pseudo triplet in a 1 : 2 : 2 intensity ratio (δ = 6.23, 6.36, and 6.76 ppm). As anticipated, in its ^{13}C NMR spectrum, seven peaks were observed, in which three peaks appeared in the aliphatic region for the isobutyl groups and four peaks in the aromatic region corresponding to the seven-membered ATI-backbone ring. Compound **2** crystallized as a tetramer, but in solution, it is a monomer, confirmed by DOSY-NMR experiment (Fig. S9). In solution, a broad singlet is observed at 2.24 ppm in the ^{27}Al NMR spectrum (Fig. S8), suggesting one type of Al(III)-centre, unlike the related compound [($Et_3SiOAlH_2$)$_2$$AlH_3$]$_2$, which has two-types of Al-centres in solution as well as in solid-state.[51] The IR-band for the Al–H bond appears at 1960 (sharp band for terminal Al–H) and 1789 (broad band for bridging Al–H) cm^{-1}, which is in good agreement with the related reported compound [($Et_3SiOAlH_2$)$_2$$AlH_3$]$_2$.[51]

After isolating compound **2** *via* the aforementioned synthetic route, the reaction between the aminotroponimine ligand (ATIH) and $Et_3N{\cdot}AlH_3$ was attempted to prepare compound **2**. However, this reaction did not yield the target product. Instead, it afforded an *N*-tetracoordinate Al(III) complex. To probe the mechanism of the formation of this *N*-tetracoordinate compound, ATIH was treated with $Et_3N{\cdot}AlH_3$ in a 2 : 1 stoichiometric ratio affording the pentacoordinated Al(III)–monohydride [(ATI)AlH(ATI)] **3**. Complex **3** eventually undergoes intramolecular hydride transfer from Al-centre to ATI-backbone to afford an *N*-tetracoordinate Al(III) complex **4** (Scheme 4). In this reaction, after 1 h, the products **3** and **4** were observed in 9 : 1 ratio (Fig. S20) and after the stirring of this reaction mixture in toluene for 12 h, compound **4** was isolated with 60% yield. This indicates that compound **3** is acting as an intermediate for the formation of compound **4**. For the isolation of compound **3**, the reaction of **2** with ATIH was also carried out to afford the desired product with 81% yield (Scheme 4). Compounds **3** and **4** are soluble in toluene and THF but insoluble in pentane. Compounds **3** and **4** were characterized by multinuclear NMR-spectroscopy and single-crystal X-ray diffraction techniques. In the ^{1}H NMR spectrum of **3**, the methyl protons appeared as a doublet at δ = 0.92 ppm, while the methine and methylene protons were observed as a multiplet (δ = 2.25–2.20 ppm) and a doublet (δ =

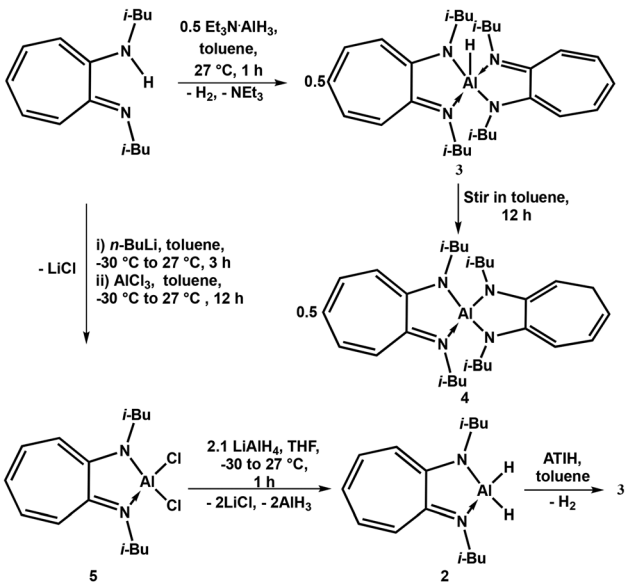

Scheme 4 Synthesis of compounds **3**–**5**.

3.39 ppm), respectively. The five protons of the seven-membered ATI backbone exhibited a triplet, doublet, and pseudo-triplet in a 1 : 2 : 2 intensity ratio at δ = 6.22, 6.58, and 6.83 ppm. The ^{13}C NMR spectrum of compound **3** showed seven distinct signals: three in the aliphatic region corresponding to the isobutyl substituents and four in the aromatic region attributable to the seven-membered ATI-ring. Compound **4** contains two ATI-ligand backbones which appear separately in the ^{1}H NMR spectrum; the resonance of methyl protons of the isobutyl-groups appeared as a pseudo triplet (δ = 0.78 ppm) and a doublet (δ = 0.89 ppm). Methine protons appeared as two multiplets (δ = 1.97–2.07 and 2.09–2.19 ppm). The methylene protons corresponding to the ^{i}Bu-groups of the non-aromatic and aromatic ligand backbone appear as two doublets (δ = 2.99 and 3.08 ppm) and one doublet (δ = 3.25 ppm), respectively. The five protons of the aromatic seven-membered ring appear as triplet, doublet, and pseudo triplet in a 1 : 2 : 2 intensity ratio (δ = 6.32, 6.66, and 6.80 ppm). The five protons of the non-aromatic seven-membered ring appear uniquely. The methylene protons of the non-aromatic seven-membered ring appeared as a triplet (δ = 2.76 ppm), the other four protons appear as a triplet, multiplets and doublet of doublets (δ = 4.76, 5.67–5.72, and 6.47 ppm). As compound **3** is asymmetric, the ^{13}C NMR spectrum shows 20 distinct resonances.

To isolate compound **2**, starting from an Al(III) precursor, Al(III)–dichloride, the reaction of aminotroponimine ligand was carried out with *n*-BuLi followed by the addition of $AlCl_3$ to afford ATI-stabilized aluminum dichloride, [(ATI)$AlCl_2$], **5** (Scheme 4). Although, the ATI-ligand has been used to isolate Al(III)–dihydride and –dimethyl,[37] compound **5** is the first example of ATI-ligand stabilized Al(III)–dihalide. Compound **5** is soluble in toluene, THF, and chloroform but insoluble in pentane. Compound **5** was characterized by multinuclear NMR spectroscopy and single-crystal X-ray diffraction techniques. In the ^{1}H NMR spectrum of compound **5**, the resonance of methyl protons appeared as a doublet (δ = 0.86 ppm). Methine and methylene protons appeared as a multiplet (δ = 2.25–2.10 ppm) and a doublet (δ = 3.16 ppm), respectively. The five protons of the seven-membered ring appear as a triplet, doublet, and pseudo triplet in a 1 : 2 : 2 intensity ratio (δ = 6.30, 6.50, and 6.73 ppm). As anticipated, seven peaks were observed in the ^{13}C NMR spectrum, in which three peaks appeared in the aliphatic region for the isobutyl groups and four peaks in the aromatic region corresponding to the seven-membered ATI-backbone ring. After isolating the desired Al(III)–dichloride **5**, its reaction with $LiAlH_4$ was performed in THF to afford compound **2** in 76% yield (Scheme 4 and Fig. S21).

To explore the reactivities of Al(III)–dihydride, **2**, the activation of the C=S bond of CS_2 was achieved by the reaction of compound **2** with CS_2 to afford ATI-stabilized Al(III)–sulfide dimer [(ATI)Al(μ-S)]$_2$ **6** as a product, with 65% yield. The activation of CS_2 by $^{Me}LAlH_2$ to afford aluminum(III) sulfide-bridged dimer [{^{Me}LAl(μ-S)}$_2$][44] proceeds through a detectable aluminum thioformate intermediate with the removal of H_2CS in the following step. Although they did not observe thioformaldehyde, they observed 1,3,5-trithianethe (at 4.17 ppm), the primary decomposition product of thioformaldehyde. In contrast, no such thioformate intermediate or 1,3,5-trithianethe was observed in the reaction of compound **2** with CS_2, as evidenced by the absence of any diagnostic thioformate or 1,3,5-trithianethe resonance in the ^{1}H NMR spectrum. However, H_2 was detected in the ^{1}H NMR spectrum (Fig. S24). A similar reaction of compound **2** with CO_2 did not yield the oxo-analogue of compound **6** but instead gave a mixture of products. Unlike $^{Me}LAlH_2$, Compound **6** can also be isolated from the reaction of compound **2** with S_8, with 85% yield. This indicates that aluminum hydride bond activations can occur *via* different mechanisms. The reaction of compound **4** with S_8 also affords compound **6** as a product (Scheme 5) (with unidentified side products), confirmed by ^{1}H NMR spectroscopy and SC-XRD analysis. The reaction of compound **4** with CS_2 gave a mixture of products.

In an effort to obtain the selenide analogue of compound **6**, compounds **2** and **4** were reacted with elemental selenium; however, no reaction occurred even upon heating up to 80 °C. Alternatively, activation of the P=Se bond in triphenylphosphine selenide ($SePPh_3$) by compound **2** afforded the Al(III) selenide dimer [(ATI)Al(μ-Se)]$_2$ **7** in 87% yield (Scheme 6). In contrast to the conversion of compound **4** to compound **6**

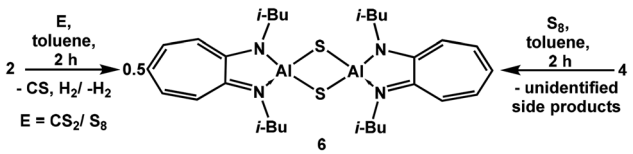

Scheme 5 Synthesis of [(ATI)Al(μ-S)]$_2$ **6**.

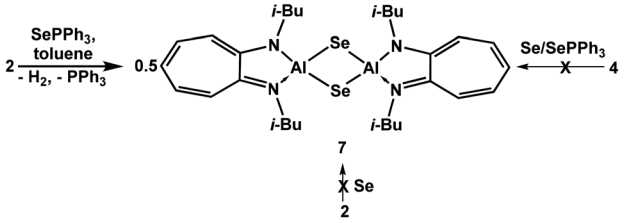

Scheme 6 Synthesis of [(ATI)Al(μ-Se)]$_2$ **7**.

shown in Scheme 5, analogous reactions of compound **4** with either selenium powder or $SePPh_3$ showed no reaction. Compounds **6** and **7** represent examples of N-heterocyclic Al(III)–chalcogenide species featuring an Al_2E_2 ring motif. Both compounds are soluble in THF but insoluble in toluene and pentane. Compounds **6** and **7** were characterized by multinuclear NMR spectroscopy and single-crystal X-ray diffraction. The ^{1}H NMR and ^{13}C NMR spectra of compounds **6** and **7** gave similar and anticipated results. For compound **6**, the resonance of methyl protons appeared as a doublet (δ = 1.08 ppm). Methine and methylene protons appeared as a multiplet (δ = 2.45–2.40 ppm) and a doublet (δ = 3.59 ppm), respectively. The five protons of the seven-membered ring appear as triplet, doublet, and pseudo triplet in a 1 : 2 : 2 intensity ratio (δ = 6.65, 6.92, and 7.25 ppm). As anticipated, in its ^{13}C NMR spectrum, seven peaks were observed, in which three peaks appeared in the aliphatic region for the isobutyl groups and four peaks in the aromatic region corresponding to the seven-membered ATI-backbone ring.

X-ray crystal structures of compounds 1–7

Single crystals of compounds **1**–**7**, suitable for single-crystal X-ray diffraction (SCXRD) studies, were grown according to the procedures described in the Experimental section. Compound **1** crystallized in the monoclinic $P2_1/n$ space group. The Si(IV)-centre in compound **1** possesses a distorted trigonal bipyramidal geometry (τ_5 = 0.75) (The τ_5 is defined as: $\tau_5 = (\beta - \alpha)/60°$. α and β refer to the two largest θ bond angles in a five-coordinate complex. In an ideal square pyramidal structure (τ_5 = 0), $\alpha = \beta$ = 180°; while in an ideal trigonal bipyramidal structure (τ_5 = 1), α = 120° and β = 180°),[52] having two N-atoms, two Cl-atoms, and one H-atom attached to it (Fig. 1). The Si–Cl bond lengths (Si1–Cl1 2.2202(6) and Si1–Cl2 2.1184(7)) in compound **1** are similar to those of related compounds;[45–49] for example, in β-diketiminate stabilized dichlorosilane [(L)SiHCl$_2$] (L = Dipp-N=CH–CH=CH–N-Dipp) the Si–Cl bond lengths are 2.192(1) and 2.091(1) Å.[46] The Si1–Cl1 bond at axial position is longer than that of the Si1–Cl2 at equatorial position as Si1–Cl1 experience greater repulsion from the three equatorial bonds.

Compound **2** crystallized as a tetramer, in the monoclinic $P2_1/c$ space group. In the molecular structure of compound **2**, two types of Al-centres are present; two (Al1 and Al1*) are penta-coordinate, having distorted square pyramidal (τ_5 = 0.16) geometry, and the other two (Al2 and Al2*) are hexacoordinated, having distorted octahedral geometry (Fig. 2). All the Al–N bond

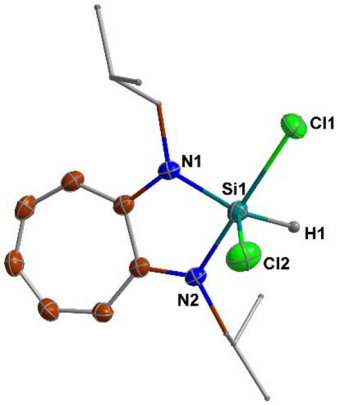

Fig. 1 Molecular structure of compound **1**: all hydrogen atoms except hydride ligand are omitted for clarity, and thermal ellipsoids are drawn at the 50% probability level. Selected bond lengths (Å) and angles (°): Si1–N1 1.793(1), Si1–N2 1.849(1), Si1–Cl1 2.2202(6), Si1–Cl2 2.1184(7), Si1–H1 1.58(3); N1–Si1–N2 84.27(6), N1–Si1–Cl1 95.54(5), N1–Si1–H1 131.00(1), Cl1–Si1–H1 86.00(1), N2–Si1–Cl1 176.15(5).

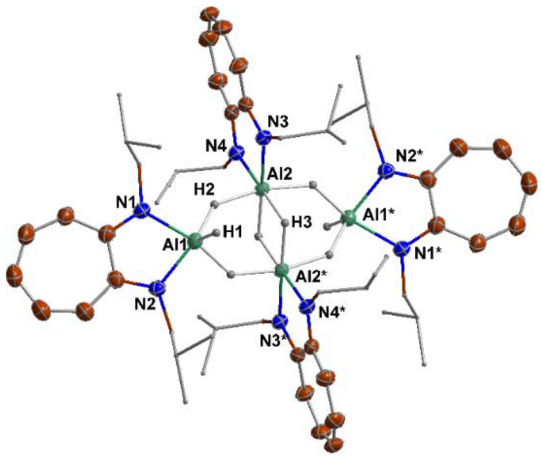

Fig. 2 Molecular structure of compound **2**: all hydrogen atoms except hydride ligands are omitted for clarity, and thermal ellipsoids are drawn at the 50% probability level. Selected bond lengths (Å) and angles (°): Al1–N1 1.916(2), Al1–N2 1.947(1), Al1–H1 1.54(2), Al1–H2 1.73(2), Al2–H2 1.74(2), Al2–N3 1.915(1), Al2–N4 1.924(2), Al2–H3 1.71(2); N1–Al1–N2 81.31(7), N3–Al1–N4 82.61(6), N1–Al1–H2 85.8(6), N2–Al1–H1 85.8(6), Al2–H3–Al2* 101(1).

lengths are similar, indicating the same oxidation state (+3) of all four Al-centres. The molecular structure of compound **2** contains two types of Al–H bonds: terminal and bridging. The bridging Al–H bond length (1.73(2) Å) is larger than the terminal one (1.54(2) Å) and are in good agreement with the related tetrameric-core in $[(Et_3SiOAlH_2)_2AlH_3]_2$ and $[H_2Al(O\text{-}C_5H_9)]_6[H(Cl)Al(O\text{-}C_5H_9)]_2$.[51,53] The molecular structure of compound **2** is the unique example of a tetrameric N-heterocyclic alane.

Compound **3** crystallized in the triclinic $P\bar{1}$ space group. In the molecular structure of the compound **3**, the Al-centre possess a distorted trigonal pyramidal geometry (τ_5 = 0.72), having four N-atoms and one H-atom attached to it (Fig. 3). As

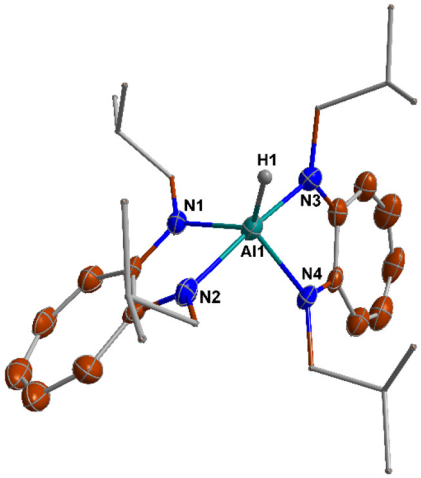

Fig. 3 Molecular structure of compound **3**: all hydrogen atoms except hydride ligand are omitted for clarity, and thermal ellipsoids are drawn at the 50% probability level. Selected bond lengths (Å) and angles (°): Al1–N1 1.942(5), Al1–N2 1.978(6), Al1–N3 1.963(6), Al1–N4 1.940(5), Al1–H1 1.62(8); N1–Al1–N2 78.8(2), N3–Al1–N4 79.8(2), N1–Al1–H1 129.00(2), N2–Al1–N3 172.0(3).

expected, the Al1–N3 and Al1–N2 bonds at the axial positions in the trigonal bipyramidal geometry are longer than the Al1–N1 and Al1–N4 bonds at the equatorial positions, as the bonds present at axial positions experience more repulsion than those present at equatorial positions in the trigonal bipyramidal geometry. The Al–H bond distance (1.62(8) Å) in **3** is between the terminal and the bridging Al–H bond distances in **2**, probably due to the difference in the coordination environment.

Compounds **4** and **5** crystallized in the monoclinic $P2_1/n$ space group. The Al(III)-centres, in compounds **4** and **5**, possess a distorted tetrahedral geometry (**4**: τ_4 = 0.83, **5**: τ_4 = 0.85) (The τ_4 is defined as: $\tau_4 = [360° - (\alpha + \beta)]/141°$. α and β refer to the two largest θ bond angles in a four-coordinate complex. In an ideal tetrahedral structure (τ_4 = 1), $\alpha = \beta$ = 109.5°, while in an ideal square planar structure (τ_4 = 0), $\alpha = \beta$ = 180°) (Fig. 4).[54] In the molecular structure of compound **4**, one of the rings has the typical geometry of a planar, aromatic aminotroponiminate-backbone and the other one is non-planar. The N3–C1 (1.404(2) Å) and N4–C5 (1.402(2) Å) bond lengths are longer than that of N1–C7 (1.350(2) Å) and N2–C6 (1.346(2) Å). In N3–C1 and N4–C5 bonds of dianionic non-aromatic ligand, there is no imine character present, while in N1–C7 and N2–C6, which are part of a monoanionic aromatic ATI-ligand, there is an imine C=N character present. As a result, the Al1–N1 (1.863(2) Å) and Al2–N2 (1.863(2) Å) bond lengths are also longer than the Al1–N3 (1.835(2) Å) and Al1–N4 (1.817 (2) Å) bond distances, which are consistent with the Al–N single bond length. The C2–C3 bond length (1.489(3) Å) is longer than the C1–C2 bond length (1.359(3) Å), indicating single-bond character for the C2–C3 bond, with a sp^3-C3 carbon. In the molecular structure of compound **5**, the bond lengths Al1–Cl1 (2.127(5) Å) and Al1–Cl2 (2.124(6) Å) are in good agreement with related compounds;[55–61] for example, β-diketiminate ligand stabilized Al(III)–dichloride [HC{C(Me)N(C_6H_3-2,6-^{i}Pr$_2$)}$_2$AlCl$_2$] has Al–Cl bond lengths of 2.1344(4) and 2.1185(4) Å.[55]

The two isostructural compounds **6** and **7** crystallize in the orthorhombic *Pbca* space group, each with a planar Al_2E_2 (E = S, Se) core (Fig. 5). In compounds **6** and **7**, the Al-centres show distorted tetrahedral geometry (**6**: τ_4 = 0.82, **7**: τ_4 = 0.83). The Al–E (E = S, Se) bond length increased as the size of the chalcogen atom increased; the Al1–S1 bond length (2.228(1) Å) in compound **6**, is slightly shorter than the Al1–Se1 bond length

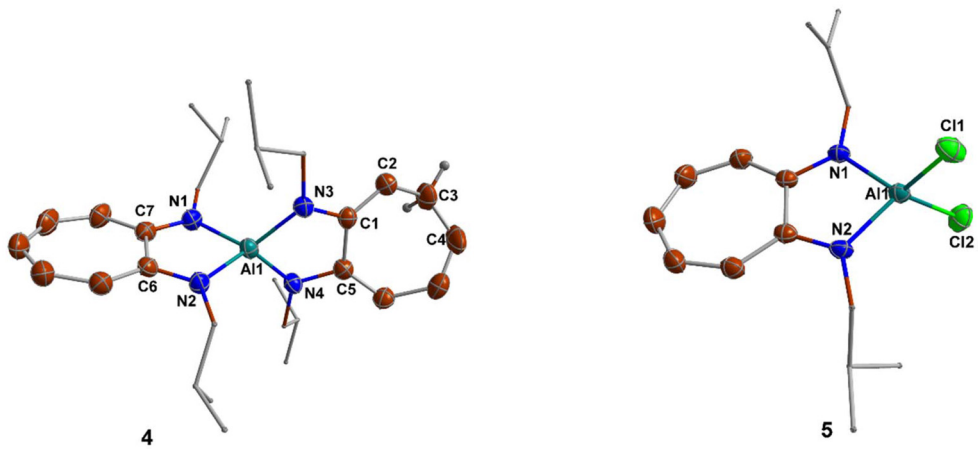

Fig. 4 Molecular structure of compound **4**: all hydrogen atoms are omitted for clarity (except methylene hydrogens in the backbone), and thermal ellipsoids are drawn at the 50% probability level. Selected bond lengths (Å) and angles (°): Al1–N1 1.876(2), Al1–N2 1.863(2), Al1–N3 1.835(2), Al1–N4 1.817(2), C1–C2 1.359(3), C2–C3 1.489(3), N3–C1 1.404(2), N4–C5 1.402(2), N1–C7 1.350(2), N2–C6 1.346(2); N1–Al1–N2 85.06(7), N3–Al1–N4 91.11 (7), N1–Al1–N3 121.86(7), N2–Al1–N4 121.82(7), C1–C2–C3 123.8(2), C2–C3–C4 117.6(2). Molecular structure of compound **5**: all hydrogen atoms are omitted for clarity, and thermal ellipsoids are drawn at the 50% probability level. Selected bond lengths (Å) and angles (°): Al1–N1 1.850(1), Al1–N2 1.846(1), Al1–Cl1 2.127(5), Al1–Cl2 2.124(6); N1–Al1–N2 87.05(6), N1–Al1–Cl1 119.41(4), N1–Al1–Cl2 110.78(4), Cl1–Al1–Cl2 107.97(2).

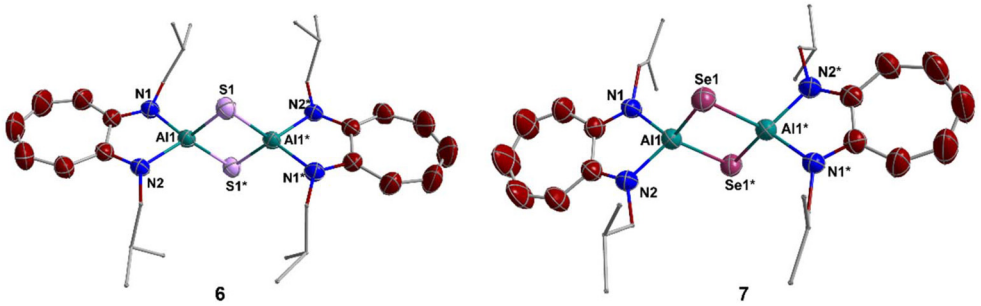

Fig. 5 Molecular structure of compound **6**: all hydrogen atoms are omitted for clarity, and thermal ellipsoids are drawn at the 50% probability level. Selected bond lengths (Å) and angles (°): Al1–N1 1.870(2), Al1–N2 1.865(2), Al1–S1 2.228(1), Al1–S1* 2.223(1); N1–Al1–N2 84.6(1), N1–Al1–S1 120.78 (8), N2–Al1–S1* 121.93(8), Al1–S1–Al1* 78.47(4), S1–Al1–S1* 101.53(4). Molecular structure of compound **7**: all hydrogen atoms are omitted for clarity, and thermal ellipsoids are drawn at the 50% probability level. Selected bond lengths (Å) and angles (°): Al1–N1 1.875(3), Al1–N2 1.875(3), Al1–Se1 2.350(1), Al1–Se2* 2.358(1); N1–Al1–N2 85.0(1), N1–Al1–Se1 114.74(9), N2–Al1–Se1* 113.16(9), Al1–Se1–Al1* 77.76(4), Se1–Al1–Se1* 102.24(4).

(2.350(1) Å) in compound **6**. Due to the chalcogen ionic radii, the S1–Al1–S1* bond angle (101.53(4)°), in compound **6**, is also smaller than the Se1–Al1–Se1* bond angle (102.24(4)°) in compound **7**. The Al–E (E = S, Se) bond distances and E–Al–E (E = S, Se) bond angles in compound **6** and **7** are similar to the related N-heterocyclic-Al_2E_2 (E = S, Se) ring containing compounds (for E = S: bond length range is 2.185(2)–2.245(1) Å and bond angle range is 96.5(1)–102.47(3)°; for E = Se: bond length range is 2.314(1)–2.381(1) Å) and bond angle range is 97.5(1)–104.5(3)°.[32,38–43] The difference in the E–Al–E bond angle range depends on the ligand backbone bulkiness.

Conclusions

In summary, we report a previously unprecedented synthetic approach that enables the isolation of the ATI-stabilized aluminum dihydride complex [(ATI)AlH_2], **2**, from Si(IV)/Ge(IV) precursors. The reactivity of compound **2** has been further demonstrated through the activation of C═S bond in CS_2 and P═Se bond in Ph_3PSe, leading to the formation of the aluminum(III) μ-sulphide dimer [(ATI)Al(μ-S)]$_2$ **6**, and the aluminum(III) μ-selenide dimer [(ATI)Al(μ-Se)]$_2$ **7**, respectively. Ongoing studies are focused on elucidating the broader reactivity and potential applications of compounds **1**–**7**.

Experimental section

General considerations

All syntheses were carried out under an N_2 atmosphere using glovebox and Schlenk techniques unless otherwise stated. All solvents used were dried by passing through a solvent purification system (MBraun, USA). Benzene-d_6 (Cambridge Isotope Laboratories) was degassed by three freeze–pump–thaw cycles and stored over a potassium mirror. ATIH ligand was synthesized as reported.[62] All ^{1}H and ^{13}C{^{1}H} spectra were taken on 300, 400 or 500 MHz Bruker spectrometers. All NMR chemical shifts are reported in ppm. ^{1}H NMR chemical shifts were referenced internally to the residual solvent peak of C_6D_6 at 7.16 ppm. ^{13}C NMR chemical shifts were referenced internally to C_6D_6 at 128.06 ppm. For ^{29}Si and ^{27}Al NMR, Et_3SiH and $AlMe_3$ have been used as an external reference, respectively. IR spectra were taken on a Nicolet Summit Pro FTIR spectrometer in transmission mode. DOSY spectra were recorded using Bruker's "ledbpgp2s" program. The gradient strength varied from 5% to 95%.

Synthesis of [(ATI)$SiHCl_2$], 1

To a solution of aminotroponimine (ATIH) (0.20 g, 0.86 mmol) in THF (20 mL), *n*-BuLi (2.5 M solution in hexane) (0.38 mL, 0.95 mmol) was added at −78 °C. After 30 minutes, the reaction mixture was slowly brought to room temperature and stirred for 3 h. This mixture was taken to −78 °C, and $SiCl_3H$ (0.096 mL, 0.946 mmol) was added. After the addition of $SiCl_3H$ was complete, the reaction mixture was brought to room temperature and stirred for 16 h. After that, THF was removed under vacuum, and the reaction mixture was extracted using toluene. The mixture was then filtered through a fine-porosity frit. Removing all volatiles from the filtrate under reduced pressure gave an orange-yellow solid. It was washed with pentane (2 × 5 mL) and dried under a vacuum to afford an analytically pure sample of compound **1** as a yellow solid. Single crystals suitable for X-ray diffraction studies were obtained from a saturated solution of compound **1** in toluene at −40 °C. Yield: 85%. ^{1}H NMR (400 MHz, C_6D_6): δ 7.05 (s, 1H, Si*H*), 6.70 (t, $^3J_{H-H}$ = 9.5 Hz, 2H, Ar*H*), 6.56 (d, $^3J_{H-H}$ = 11.1 Hz, 2H, Ar*H*), 6.30 (t, $^3J_{H-H}$ = 9.4 Hz, 1H, Ar*H*), 3.61 (d, $^3J_{H-H}$ = 7.4 Hz, 4H, CH_2), 2.06–2.00 (m, 2H, $(CH_3)_2CH$), 0.82 (d, $^3J_{H-H}$ = 6.7 Hz, 12H, CH_3). ^{29}Si{^{1}H} NMR (79.5 MHz, C_6D_6): δ −88.2 (s, *Si*–H). ^{29}Si NMR (60 MHz, C_6D_6): δ −88.0 (d, $^2J_{Si-H}$ = 347.0 Hz, *Si*–H). ^{13}C{^{1}H} NMR (101 MHz, C_6D_6): δ 155.2, 137.8, 125.3, 118.2, 52.2, 27.1, 20.8 ppm. IR: ν(Si–H) = 2357 and 2338 cm^{-1}.

Synthesis of [(ATI)AlH_2], 2

To the solution of compound **1** (0.20 g, 0.60 mmol) in diethyl ether (10 mL), $LiAlH_4$ (0.07 g, 1.8 mmol) was added at −30 °C, and the reaction mixture was allowed to be stirred for 2 h at

room temperature. After that, the reaction mixture was filtered through a fine-porosity frit. The solvent was removed under reduced pressure, and the remaining solid was extracted in toluene. This solution was concentrated and kept at −30 °C in the freezer to afford analytically pure, yellow-colored crystals of compound **2**. Yield: 68%. ^{1}H NMR (400 MHz, C_6D_6): δ 6.76 (t, $^3J_{H-H}$ = 10.2 Hz, 2H, Ar*H*), 6.36 (d, $^3J_{H-H}$ = 11.1 Hz, 2H, Ar*H*), 6.23 (t, $^3J_{H-H}$ = 9.3 Hz, 1H, Ar*H*), 5.06 (s, 2H, Al*H*), 3.00 (d, $^3J_{H-H}$ = 6.9 Hz, 4H, CH_2), 2.19–2.13 (m, 2H, $(CH_3)_2CH$), 0.92 (d, $^3J_{H-H}$ = 6.5 Hz, 12H, CH_3).^{13}C NMR (101 MHz, C_6D_6): δ 162.9, 136.7, 120.1, 114.4, 55.4, 28.6, 21.5. ^{27}Al NMR (130.3 MHz, C_6D_6, 298 K): 2.24 (s, broad). IR: ν(Al–H) = 1760 (sharp, Al–H, terminal), 1789 (broad, Al–H, bridging) cm^{-1}.

Synthesis of [(ATI)AlH(ATI)], 3

To a solution of **2** (0.030 g, 0.11 mmol) in toluene (5 mL), toluene (2 mL) solution of ATIH (0.0267 g, 0.11 mmol) was added, and the reaction mixture was stirred for 0.5 h. After that, the solvent was removed under reduced pressure to obtain a yellow solid compound. This solid was washed with pentane (2 × 2 mL) to afford analytically pure yellow compound **3**. Single crystals suitable for X-ray diffraction studies were obtained from a saturated solution of compound **3** in toluene at −30 °C. Yield: 81%. ^{1}H NMR (500 MHz, C_6D_6): δ 6.83 (t, $^3J_{H-H}$ = 10.1 Hz, 2H, Ar*H*), 6.58 (d, $^3J_{H-H}$ = 11.3 Hz, 2H, Ar*H*), 6.22 (t, $^3J_{H-H}$ = 9.1 Hz, 1H, Ar*H*), 5.32 (s, very broad, Al–*H*), 3.39 (d, $^3J_{H-H}$ = 7.0 Hz, 4H, CH_2), 2.25–2.2 (m, 2H, $(CH_3)_2CH$), 0.92 (d, $^3J_{H-H}$ = 6.6 Hz, 12H, CH_3) ppm.^{13}C NMR (125 MHz, C_6D_6): δ 161.4, 135.3, 118.2, 113.9, 54.2, 26.9, 21.4. IR: ν(Al–H) = 1705 (weak, broad, Al–H) cm^{-1}.

Synthesis of [(ATI)Al(ATIH)], 4

To a solution of ATIH (0.098 g, 0.42 mmol) in toluene (5 mL), toluene (2 mL) solution of $Et_3N{\cdot}AlH_3$ (0.0276 g, 0.21 mmol) was added, and the reaction mixture was stirred for 1 h and after evaporation of toluene ~91% of **3** and ~9% of **4** was observed in ^{1}H NMR spectrum. This solid reaction mixture was further dissolved in toluene, giving a yellowish-orange solution, and stirred for 12 h to give a reddish-yellow solution. After that, the solvent was removed under reduced pressure to obtain a reddish-yellow solid compound. This solid was washed with pentane (3 × 2 mL) to afford analytically pure reddish-yellow compound **4**. Single crystals suitable for X-ray diffraction studies were obtained from a saturated solution of compound **4** in toluene at −30 °C. Yield: 60%. ^{1}H NMR (400 MHz, C_6D_6): δ 6.80 (t, $^3J_{H-H}$ = 9.5 Hz, 2H, Ar*H*), 6.66 (d, $^3J_{H-H}$ = 11.3 Hz, 2H, Ar*H*), 6.47 (dd, $^3J_{H-H}$ = 9.2, 6.5 Hz, 1H, *n*-Ar*H*), 6.32 (t, $^3J_{H-H}$ = 9.2 Hz, 1H, Ar*H*), 5.72–5.67 (m, 2H, *n*-Ar*H*), 4.76 (t, $^3J_{H-H}$ = 7.3 Hz, 1H, *n*-Ar*H*), 3.25 (d, $^3J_{H-H}$ = 6.9 Hz, 4H, (*i*-Bu)CH_2), 3.08 (d, $^3J_{H-H}$ = 6.5 Hz, 2H, (*i*-Bu)CH_2), 2.99 (d, $^3J_{H-H}$ = 6.3 Hz, 2H, (*i*-Bu)CH_2), 2.76 (t, $^3J_{H-H}$ = 6.9 Hz, 2H, -ArCH_2), 2.19–2.09 (m, 2H, (*i*-Bu)C*H*), 2.07–1.97 (m, 2H, (*i*-Bu)C*H*), 0.91 (d, $^3J_{H-H}$ = 6.6 Hz, 6H, CH_3), 0.89 (d, $^3J_{H-H}$ = 6.6 Hz, 6H, CH_3), 0.78 (t, $^3J_{H-H}$ = 6.3 Hz, 12H, CH_3) ppm. ^{13}C{^{1}H} NMR (101 MHz, C_6D_6): ^{13}C NMR (101 MHz, C_6D_6): δ 161.2, 154.2, 149.2, 136.7, 126.8, 122.5, 116.2, 115.8, 99.2, 90.2, 56.1, 55.3, 55.1, 28.3, 27.8, 27.1, 26.7, 22.0, 21.9, 21.2 ppm.

Synthesis of [(ATI)AlCl$_2$], 5

To a solution of aminotroponimine (ATIH) (0.20 g, 0.86 mmol) in toluene (20 mL), *n*-BuLi (2.5 M solution in hexane) (0.38 mL, 0.95 mmol) was added at −30 °C and stirred for 3 h at room temperature. To this reaction mixture, toluene suspension of $AlCl_3$ (0.114 g, 0.86 mmol) was added at −30 °C, and the reaction mixture was stirred at room temperature for 2 h. After the reaction time, the yellow-coloured toluene solution was carefully transferred (leaving the settled oily side product) to a fine-porosity frit and filtered. Removing all volatiles from the filtrate under reduced pressure gave a yellow solid. It was washed with pentane (3 × 5 mL) and dried under a vacuum to afford an analytically pure sample of compound **5** as a yellow solid. Single crystals suitable for X-ray diffraction studies were obtained from a saturated solution of compound **5** in toluene at −30 °C. Yield: 62%. ^{1}H NMR (400 MHz, C_6D_6): δ 6.73 (t, $^3J_{H-H}$ = 10.2 Hz, 2H, Ar*H*), 6.50 (d, $^3J_{H-H}$ = 11.2 Hz, 2H, Ar*H*), 6.30 (t, $^3J_{H-H}$ = 9.3 Hz, 1H, Ar*H*), 3.16 (d, $^3J_{H-H}$ = 7.1 Hz, 4H, CH_2), 2.25–2.10 (m, 2H, $(CH_3)_2CH$), 0.86 (d, $^3J_{H-H}$ = 6.6 Hz, 12H, CH_3). ^{13}C NMR (125 MHz, C_6D_6): δ 161.1, 137.1, 123.3, 116.26, 54.3, 28.1, 21.2.

Synthesis of [(ATI)Al(μ-S)]$_2$, 6

To a solution of compound **2** (0.10, 0.38 mmol) in toluene (5 mL), CS_2 (0.028 mL, 0.58 mmol) was added, and the reaction mixture was stirred for 2 h. After the reaction time, a yellow-coloured precipitate formed. The reaction mixture was filtered through a fine-porosity frit, and the residue was washed with toluene (2 × 2 mL). The residue was collected, dissolved in THF to form a saturated solution, and stored at −30 °C to afford analytically pure, yellow-colored crystals of compound **6**. Yield: 65%. ^{1}H NMR (500 MHz, $CDCl_3$): δ 7.25 (t, $^3J_{H-H}$ = 10.2 Hz, 4H, Ar*H*), 6.92 (d, $^3J_{H-H}$ = 11.3 Hz, 4H, Ar*H*), 6.65 (t, $^3J_{H-H}$ = 9.4 Hz, 2H, Ar*H*), 3.59 (d, $^3J_{H-H}$ = 7.3 Hz, 8H, CH_2), 2.45–2.40 (m, 4H, $(CH_3)_2CH$), 1.08 (d, $^3J_{H-H}$ = 6.6 Hz, 24H, CH_3). ^{13}C NMR (101 MHz, $CDCl_3$): δ 161.2, 136.5, 121.8, 115.3, 54.0, 27.8, 21.7.

Synthesis of [(ATI)Al(μ-Se)]$_2$, 7

To a solution of compound **2** (0.10, 0.38 mmol) in toluene (5 mL), $SePPh_3$ (0.13 g, 0.38 mmol) was added, and the reaction mixture was stirred for 2 h. After the reaction time, a yellow-coloured precipitate formed. The reaction mixture was filtered through a fine-porosity frit, and the residue was washed with toluene (2 × 2 mL). The residue was then collected, and the residual solvent was removed under reduced pressure to afford a yellow-colored analytically pure compound **7**. Single crystals suitable for X-ray diffraction studies were obtained from a saturated solution of compound **7** in THF at −30 °C. Yield: 87%. ^{1}H NMR (500 MHz, $CDCl_3$): δ 7.25 (t, $^3J_{H-H}$ = 10.2 Hz, 4H, Ar*H*), 6.91 (d, $^3J_{H-H}$ = 11.3 Hz, 4H, Ar*H*), 6.63 (t, $^3J_{H-H}$ = 9.3 Hz, 2H, Ar*H*), 3.61 (d, $^3J_{H-H}$ = 7.2 Hz, 8H, CH_2), 2.53–2.43 (m, 4H, $(CH_3)_2CH$), 1.09 (d, $^3J_{H-H}$ = 6.6 Hz, 24H, CH_3). ^{13}C NMR (101 MHz, $CDCl_3$): δ 161.0, 136.4, 121.9, 115.6,

53.9, 27.9, 21.8 ppm. ^{77}Se NMR: Not observed (range attempted: 1000 to −880 ppm).

Conflicts of interest

There are no conflicts to declare.

Data availability

The data supporting this article have been included as part of the supplementary information (SI). Supplementary information: NMR spectra and DOSY NMR experiment and IR spectra. See DOI: https://doi.org/10.1039/d6dt00474a.

CCDC 2532228–2532233, 2538185 (**1–7**) contain the supplementary crystallographic data for this paper.[63a–g]

Acknowledgements

J. R. W. gratefully acknowledges the Department of Energy, Office of Basic Energy Sciences, Heavy Element Program under Award DE-SC0021273. H. K. gratefully acknowledges the MU College of Arts & Science and Department of Chemistry for postdoctoral funding. S. N. thanks the SERB, Department of Science and Technology (DST), New Delhi, India, for funding (CRG/2022/005756).

References

1 W. Grochala and P. P. Edwards, *Chem. Rev.*, 2004, **104**, 1283–1316.
2 S. Harder, *Chem. Commun.*, 2012, **48**, 11165.
3 M. M. D. Roy, A. A. Omaña, A. S. S. Wilson, M. S. Hill, S. Aldridge and E. Rivard, *Chem. Rev.*, 2021, **121**, 12784–12965.
4 S. Aldridge and A. J. Downs, *Chem. Rev.*, 2001, **101**, 3305–3366.
5 T. He, H. Cao and P. Chen, *Adv. Mater.*, 2019, **31**, 1902757.
6 S. Goswami, P. Mandal, S. Sarkar, M. Mukherjee, S. Pal, D. Mallick and D. Mukherjee, *Dalton Trans.*, 2024, **53**, 1346–1354.
7 C. Mandal, A. Kundu, S. Das, D. Adhikari and D. Mukherjee, *Chem. – Eur. J.*, 2023, **29**, e202301119.
8 Z. Yang, M. Zhong, X. Ma, K. Nijesh, S. De, P. Parameswaran and H. W. Roesky, *J. Am. Chem. Soc.*, 2016, **138**, 2548–2551.
9 C.-C. Chia, Y.-C. Teo, N. Cham, S. Y.-F. Ho, Z.-H. Ng, H.-M. Toh, N. Mézailles and C.-W. So, *Inorg. Chem.*, 2021, **60**, 4569–4577.
10 (*a*) Z. Pang, X. Ma, W. Yan, X. Yang, C. Ni, Y. Chen, P. Wu and Z. Yang, *Inorg. Chem. Front.*, 2025, **12**, 2772–2782; (*b*) M. De Vere-Tucker, I. Squire, M. Tritto, R. Anandkar, T. Syeda, D. Uthayan, G. Aguila, L. Silva de Moraes and C. Bakewell, *Dalton Trans.*, 2026, **55**, 4977–4987, DOI: 10.1039.D6DT00276E.
11 K. Hobson, C. J. Carmalt and C. Bakewell, *Inorg. Chem.*, 2021, **60**, 10958–10969.
12 T. W. Myers and L. A. Berben, *J. Am. Chem. Soc.*, 2013, **135**, 9988–9990.
13 R. L. Falconer, G. S. Nichol and M. J. Cowley, *Inorg. Chem.*, 2019, **58**, 11439–11448.
14 Y.-L. Lien, Y.-C. Chang, N.-T. Chuang, A. Datta, S.-J. Chen, C.-H. Hu, W.-Y. Huang, C.-H. Lin and J.-H. Huang, *Inorg. Chem.*, 2010, **49**, 136–143.
15 T. W. Myers and L. A. Berben, *Chem. Sci.*, 2014, **5**, 2771–2777.
16 P.-Y. Lee and L.-C. Liang, *Inorg. Chem.*, 2009, **48**, 5480–5487.
17 B. Luo, B. E. Kucera and W. L. Gladfelter, *Dalton Trans.*, 2006, 4491.
18 A. H. Cowley, F. P. Gabbaï, H. S. Isom and A. Decken, *J. Organomet. Chem.*, 1995, **500**, 81–88.
19 J.-C. Chang, C.-H. Hung and J.-H. Huang, *Organometallics*, 2001, **20**, 4445–4447.
20 T. S. Koptseva, E. V. Baranov, S. Yu. Ketkov and I. L. Fedushkin, *Inorg. Chem. Front.*, 2026, **13**, 3070–3078.
21 C. Mandal, A. Kundu, S. Panda and D. Mukherjee, *Chem. Commun.*, 2026, **62**, 869–873.
22 M. L. Cole, A. J. Davies, C. Jones, P. C. Junk, A. I. McKay and A. Stasch, *Z. Anorg. Allg. Chem.*, 2015, **641**, 2233–2244.
23 S. González-Gallardo, V. Jancik, R. Cea-Olivares, R. A. Toscano and M. Moya-Cabrera, *Angew. Chem., Int. Ed.*, 2007, **46**, 2895–2898.
24 C. Sindlinger, S. Lawrence, D. Cordes, A. Slawin and A. Stasch, *Inorganics*, 2017, **5**, 29.
25 M. L. Cole, C. Jones, P. C. Junk, M. Kloth and A. Stasch, *Chem. – Eur. J.*, 2005, **11**, 4482–4491.
26 C. G. Gianopoulos, K. Kirschbaum and M. R. Mason, *Organometallics*, 2014, **33**, 4503–4511.
27 X. Wang, F. Rüttger, A. Krawczuk, R. Herbst-Irmer and D. Stalke, *Eur. J. Inorg. Chem.*, 2024, **27**, e202300629.
28 W. Uhl and B. Jana, *Chem. – Eur. J.*, 2008, **14**, 3067–3071.
29 N. Kuhn, S. Fuchs and M. Steimann, *Z. Anorg. Allg. Chem.*, 2000, **626**, 1387–1392.
30 N. Sarkar, S. Bera and S. Nembenna, *J. Org. Chem.*, 2020, **85**, 4999–5009.
31 A. E. Nako, S. J. Gates, A. J. P. White and M. R. Crimmin, *Dalton Trans.*, 2013, **42**, 15199.
32 V. Jancik, M. M. Moya Cabrera, H. W. Roesky, R. Herbst-Irmer, D. Neculai, A. M. Neculai, M. Noltemeyer and H. Schmidt, *Eur. J. Inorg. Chem.*, 2004, **2004**, 3508–3512.
33 Y. Yang, H. Li, C. Wang and H. W. Roesky, *Inorg. Chem.*, 2012, **51**, 2204–2211.
34 S. Ito, K. Tanaka and Y. Chujo, *Inorganics*, 2019, **7**, 100.
35 M. L. Tarlton, S. P. Kelley and J. R. Walensky, *Acta Crystallogr., Sect. E: Crystallogr. Commun.*, 2021, **77**, 1258–1262.
36 H. Kumar, S. P. Kelley, T. Batra, S. Nagendran and J. R. Walensky, *Z. Anorg. Allg. Chem.*, 2026, e202500231.

37 H. V. R. Dias, W. Jin and R. E. Ratcliff, *Inorg. Chem.*, 1995, **34**, 6100–6105.
38 M. Zhong, Y. Liu, X. Liu, X. Ma and Z. Yang, *Inorg. Chim. Acta*, 2017, **464**, 182–185.
39 C. Cui, H. W. Roesky, M. Noltemeyer and H.-G. Schmidt, *Organometallics*, 1999, **18**, 5120–5123.
40 Y. Peng, H. Hao, V. Jancik, H. W. Roesky, R. Herbst-Irmer and J. Magull, *Dalton Trans.*, 2004, 3548.
41 S. González-Gallardo, A. S. Cruz-Zavala, V. Jancik, F. Cortés-Guzmán and M. Moya-Cabrera, *Inorg. Chem.*, 2013, **52**, 2793–2795.
42 H. Zhu, J. Chai, H. W. Roesky, M. Noltemeyer, H. Schmidt, D. Vidovic and J. Magull, *Eur. J. Inorg. Chem.*, 2003, **2003**, 3113–3119.
43 M. Dehmel, A. Köhler, H. Görls and R. Kretschmer, *Dalton Trans.*, 2021, **50**, 8434–8445.
44 S. González-Gallardo, V. Jancik, D. G. Díaz-Gómez, F. Cortés-Guzmán, U. Hernández-Balderas and M. Moya-Cabrera, *Dalton Trans.*, 2019, **48**, 5595–5603.
45 F. M. Mück, K. Junold, J. A. Baus, C. Burschka and R. Tacke, *Eur. J. Inorg. Chem.*, 2013, **2013**, 5821–5825.
46 Y. Xiong, S. Yao, A. Kostenko and M. Driess, *Dalton Trans.*, 2018, **47**, 2152–2155.
47 S. Takahashi, J. Sekiguchi, A. Ishii and N. Nakata, *Angew. Chem., Int. Ed.*, 2021, **60**, 4055–4059.
48 P. Garg, D. Dange and C. Jones, *Eur. J. Inorg. Chem.*, 2020, **2020**, 4037–4044.
49 S. Takahashi, A. Ishii and N. Nakata, *Chem. Commun.*, 2021, **57**, 6728–6731.
50 B. Blom, M. Pohl, G. Tan, D. Gallego and M. Driess, *Organometallics*, 2014, **33**, 5272–5282.
51 M. Veith, J. Frères, V. Huch and M. Zimmer, *Organometallics*, 2006, **25**, 1875–1880.
52 A. G. Blackman, E. B. Schenk, R. E. Jelley, E. H. Krenske and L. R. Gahan, *Dalton Trans.*, 2020, **49**, 14798–14806.
53 A. A. Ali, V. Huch, C. Aktas and M. Veith, *Z. Anorg. Allg. Chem.*, 2016, **642**, 973–978.
54 L. Yang, D. R. Powell and R. P. Houser, *Dalton Trans.*, 2007, 955–964.
55 M. Stender, B. E. Eichler, N. J. Hardman, P. P. Power, J. Prust, M. Noltemeyer and H. W. Roesky, *Inorg. Chem.*, 2001, **40**, 2794–2799.
56 M. E. Desat and R. Kretschmer, *Inorg. Chem.*, 2019, **58**, 16302–16311.
57 M. S. Hill, P. B. Hitchcock and S. M. A. Karagouni, *J. Organomet. Chem.*, 2004, **689**, 722–730.
58 X. Liu, H. Xia, W. Gao, L. Ye, Y. Mu, Q. Su and Y. Ren, *Eur. J. Inorg. Chem.*, 2006, **2006**, 1216–1222.
59 B. E. Cole, J. P. Wolbach, W. G. Dougherty, N. A. Piro, W. S. Kassel and C. R. Graves, *Inorg. Chem.*, 2014, **53**, 3899–3906.
60 Y. Cheng, D. J. Doyle, P. B. Hitchcock and M. F. Lappert, *Dalton Trans.*, 2006, 4449–4460.
61 S. Dagorne, S. Bellemin-Laponnaz and R. Welter, *Organometallics*, 2004, **23**, 3053–3061.
62 S. Sinhababu, R. K. Siwatch, G. Mukherjee, G. Rajaraman and S. Nagendran, *Inorg. Chem.*, 2012, **51**, 9240–9248.
63 (*a*) CCDC 2532228: Experimental Crystal Structure Determination, 2026, DOI: 10.5517/ccdc.csd.cc2qzzsh; (*b*) CCDC 2532229: Experimental Crystal Structure Determination, 2026, DOI: 10.5517/ccdc.csd.cc2qzztj; (*c*) CCDC 2532230: Experimental Crystal Structure Determination, 2026, DOI: 10.5517/ccdc.csd.cc2qzzvk; (*d*) CCDC 2532231: Experimental Crystal Structure Determination, 2026, DOI: 10.5517/ccdc.csd.cc2qzzwl; (*e*) CCDC 2532232: Experimental Crystal Structure Determination, 2026, DOI: 10.5517/ccdc.csd.cc2qzzxm; (*f*) CCDC 2532233: Experimental Crystal Structure Determination, 2026, DOI: 10.5517/ccdc.csd.cc2qzzyn; (*g*) CCDC 2538185: Experimental Crystal Structure Determination, 2026, DOI: 10.5517/ccdc.csd.cc2r65y3.